Article

Chinese Science Bulletin

Cell Biology

December 2011 Vol.56 No.35: 3829–3835
doi: 10.1007/s11434-011-4789-0

Detecting CD20-Rituximab interaction forces using AFM single-molecule force spectroscopy

LI Mi[1,2], LIU LianQing[1*], XI Ning[1,3*], WANG YueChao[1], DONG ZaiLi[1], LI GuangYong[1,4], XIAO XiuBin[5] & ZHANG WeiJing[5*]

[1] *State Key Laboratory of Robotics, Shenyang Institute of Automation, Chinese Academy of Sciences, Shenyang 110016, China;*
[2] *Graduate University of Chinese Academy of Sciences, Beijing 100049, China;*
[3] *Department of Electrical and Computer Engineering, Michigan State University, East Lansing 48824, USA;*
[4] *Department of Electrical and Computer Engineering, University of Pittsburgh, Pittsburgh 15261, USA;*
[5] *Department of Lymphoma, Affiliated Hospital of Military Medical Academy of Sciences, Beijing 100071, China*

Received June 11, 2011; accepted August 22, 2011

The invention of atomic force microscopy (AFM) has provided new technology for measuring specific molecular interaction forces. Using AFM single-molecule force spectroscopy (SMFS) techniques, CD20-Rituximab rupture forces were measured on purified CD20 proteins, Raji cells, and lymphoma patient B cells. Rituximab molecules were linked onto AFM tips using AFM probe functionalization technology, and purified CD20 proteins were attached to mica using substrate functionalization technology. Raji cells (a lymphoma cell line) or lymphoma patient cells were immobilized on a glass substrate via electrostatic adsorption and chemical fixation. The topography of the purified CD20 proteins, Raji cells, and patient lymphoma cells was visualized using AFM imaging and the differences in the rupture forces were analyzed and measured. The results showed that the rupture forces between the CD20 proteins on Raji cells and Rituximab were markedly smaller than those for purified CD20 proteins and CD20 proteins on lymphoma patient B cells. These findings provide an effective experimental method for investigating the mechanisms underlying the variable efficacy of Rituximab.

atomic force microscopy, single-molecule force spectroscopy, non-Hodgkin's lymphoma, monoclonal antibody

Citation: Li M, Liu L Q, Xi N, et al. Detecting CD20-Rituximab interaction forces using AFM single-molecule force spectroscopy. Chinese Sci Bull, 2011, 56: 3829–3835, doi: 10.1007/s11434-011-4789-0

The invention of atomic force microscopy (AFM) [1] allows researchers to investigate the topographical structure and specific molecular interactions between individual live cells and molecules, thereby revolutionizing the research methods used in the field of life sciences. The resolution of light microscopy is limited to the wavelength of the light source and, therefore, information on a nanometer scale is not accessible; also, electron microscopy requires vacuum conditions, which means that live samples cannot be examined using this technique [2]. Compared with light microscopy and electron microscopy, AFM has sub-nanometer resolution [3], can work under various conditions such as air, liquid, and/or a vacuum, and allows the visualization of live cells and native biomolecules without the need for staining or fixation [4]. These advantages make AFM widely applicable to life sciences, a field in which research into individual cells/molecules using AFM is at the frontier [5–7].

As a result of significant advances over the last two decades, AFM has evolved into a multifunctional tool [4]. Chemical treatment of the AFM tip and substrate allows the measurement of specific protein-protein binding forces using the force curve mode, a technique known as single-molecule force spectroscopy (SMFS) [8]. In SMFS, ligands/antibodies are linked to AFM tips and receptors/antigens are then bound to a substrate. Using the functionalized tip to obtain force curves for the protein-coated

*Corresponding authors (email: lqliu@sia.cn; xin@egr.msu.edu; zhangwj3072@163.com)

substrate, the rupture forces between the antibody-antigen/receptor-ligand can be measured. SMFS was first used in the mid-1990s. Florin et al. [9] measured the rupture force for the biotin-avidin complex immobilized on biotinylated agarose beads by linking avidin to the AFM tip. Hinterdorfer et al. [10] measured the rupture force between human serum albumin (HSA) and anti-HSA by linking the anti-HSA onto an AFM tip using polyethylene glycol (PEG) linker molecules and linking HSA onto mica surfaces. In addition to measuring the molecular forces between protein-coated substrates, SMFS can also measure molecular forces at the cell surface. Puntheeranurak et al. [11] measured the specific binding forces between the Na^+-glucose co-transporter (SGLT1) to its antibodies on Chinese hamster ovary (CHO) cells, and Shi et al. [12] investigated the interaction forces between Heregulin and HER3 on human embryonic kidney (HEK) 293 cells.

The clinical application of Rituximab (a monoclonal antibody against CD20) during the last decade has highlighted a marked difference in efficacy in the treatment of patients with non-Hodgkin's lymphoma [13]. The target of Rituximab is the CD20 antigen, which is a tetra-spanning membrane protein expressed on mature B cells and by most B cell lymphomas [14]. After binding to CD20 on the cell surface, Rituximab induces target cell lysis via antibody-dependent cellular cytotoxicity (ADCC), complement-dependent cytotoxicity (CDC), and programmed cell death (PCD) [15]. Rituximab achieved unprecedented success and, particularly in combination with chemotherapy, significantly improved the survival rates of lymphoma patients [16]. However, owing to its varying efficacy in different patients, there is an urgent need for improvement [13]. A better understanding of the mechanisms underlying Rituximab-mediated cell death should make it possible to develop new and more effective therapeutic agents [17]. In the present study, the specific CD20-Rituximab recognition interactions were investigated, and the rupture forces between Rituximab and purified CD20 proteins, CD20 proteins expressed by Raji cells, and CD20 proteins expressed by lymphoma patient B cells were measured using SMFS. The results may pave the way for further investigations into the relationship between the variable efficacy of Rituximab and CD20-Rituximab interaction forces.

1 Principle

The principle behind measuring the CD20-Rituximab rupture forces is shown in Figure 1. Rituximab was linked onto the AFM tip via a PEG linker molecule. To measure the rupture forces between the purified CD20 proteins and Rituximab, the CD20 proteins were attached to a mica substrate (Figure 1(a)). When measuring the rupture forces between Rituximab and the CD20 proteins expressed on lymphoma cells, lymphoma cells were immobilized on a glass surface via electrostatic adsorption and chemical fixation (Figure 1(b)). During the force curve mode, the probe slowly approaches and contacts the substrate/cell, causing the Rituximab molecules on the tip to bind to the CD20 molecules on the substrate/cell and form CD20-Rituximab complexes. The probe then retracts from the substrate/cell. The CD20-Rituximab complexes dissociate when the force exerted by the probe is equal to the CD20-Rituximab rupture force. By recording the displacement of the piezo tube and the deflection of the probe cantilever during the approach-retract cycle, force-distance curves can be constructed (Figure 1(c)). Each force curve comprises two portions: the approach curve and the retract curve. If the CD20-Rituximab binding events occur during the approach, there is an abrupt peak in the retract portion of the force curve. The abrupt peak corresponds to the dissociation of the CD20-Rituximab complexes. By analyzing these force curves, individual CD20-Rituximab rupture forces can be calculated.

2 Materials and methods

2.1 Materials

Rituximab (10 mg/mL) was obtained from the Chinese Affiliated Hospital of the Military Medical Academy of Sciences. *N*-hydroxysuccinimide-polyethylene glycol-Maleimide (NHS-PEG-MAL, MW 2000) was purchased from JenKem (China). Functionalization reagents were purchased from

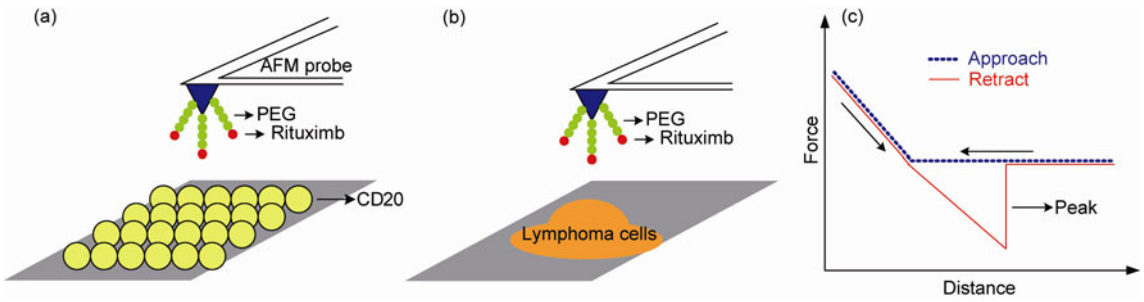

Figure 1 Principles behind the measurement of CD20-Rituximab rupture forces using SMFS. (a) Measuring the forces on purified CD20 proteins. (b) Measuring the forces on lymphoma cells. (c) The force curve.

Sigma-Aldrich (USA), including aminopropyltriethoxysilane (APTES), N,N-diisopropylethylamine, triethylamine, and phosphate buffered saline (PBS), or from J & K (China), including hydroxylamine, chloroform, dimethyl sulfoxide (DMSO), and *N*-Succinimidyl 3-(Acetylthio) propionate (SATP). Poly-*L*-lysine and glutaraldehyde were purchased from Solarbio Science and Technology Co. (China). CD20 proteins were purchased from Huaruikang Company (China). Milli-Q ultra-pure water (18.2 MΩ cm) was used for all experiments.

2.2 Protein and cell immobilization

CD20 proteins were attached to freshly cleaved mica (1 cm × 1 cm squares) according to established procedures [18]. A glass desiccator was purged with argon for 2 min. APTES (30 μL) was pipetted into a small petri dish and *N*,*N*-diisopropylethylamine (10 μL) was pipetted into another small petri dish. The freshly cleaved mica and the two petri dishes were placed in the glass desiccator, purged with argon for 2 min, and sealed for 0.5–2 h to allow the APTES vapor to mix with the *N*,*N*-diisopropylethylamine vapor and coat a layer of $-NH_2$ onto the AFM probe surface. Glutaraldehyde solution (200 μL) was then added to the mica and incubated for 10 min (the glutaraldehyde reacts with the NH_2 on the tip surface) [18]. The mica was then rinsed with Milli-Q ultra-pure water. CD20 protein solution (100 μL) was added to the mica and incubated for 30 min. The mica was then rinsed with Milli-Q ultra-pure water again and placed in a petri dish with PBS prior to probing by AFM.

Raji cells (a Burkitt's lymphoma cell line) were cultured in RPMI-1640 culture medium containing 10% fetal bovine serum at 37°C (in 5% CO_2). The cells were attached to glass slides via poly-*L*-lysine-induced electrostatic adsorption and glutaraldehyde chemical fixation. In brief, the glass slides were coated with poly-*L*-lysine and stored at room temperature overnight. Cells were harvested by centrifuging at 1000 r/min and a drop of the cell suspension placed onto a glass slide. After 30 min, the cells were fixed with 0.25% glutaraldehyde for 15 min and the slide placed in a petri dish with PBS for the AFM experiments.

Lymphoma patient samples were prepared from the bone marrow of a B lymphoma patient. A paracentesis needle was used to acquire the bone marrow, which was then added to the poly-*L*-lysine-coated glass slides. A fresh glass slide was used to disperse the bone marrow and 4% formaldehyde was used for chemical fixation.

2.3 Probe functionalization

The heterobifunctional linker, NHS-PEG-MAL, was used to tether Rituximab to the AFM stylus. This linker contains an NHS ester at one end and a MAL ester at the other. The stylus functionalization process followed was performed according to established procedures [19]. APTES (30 μL) and *N*,*N*-diisopropylethylamine (10 μL) were used to coat the AFM stylus with $-NH_2$ groups under argon gas in a glass desiccator for 0.5–2 h. The PEG linker and triethylamine were mixed in chloroform and then incubated with the NH_2-modified probes for 2–3 h. Rituximab was treated with SATP to form thiol functional groups (the thiols react with the MAL end of the PEG linker) [20]. Finally the probes were placed in the SATP-Rituximab mixture containing hydroxylamine and buffer solution (pH 7.5) for 1 h. The functionalized probes were stored in PBS at 4°C.

2.4 AFM imaging and measurements

AFM imaging and measurements were performed using a Dimension 3100 AFM and a MultiMode AFM (Veeco AFM, Santa Barbara, CA, USA) with silicon nitride probes (0.06 N/m). The spring constant was calibrated using a Thermal Tune Adapter (Veeco AFM). All experiments were performed in PBS at room temperature. Non-functionalized probes were used to visualize the topography of the CD20 proteins (MultiMode AFM), lymphoma Raji cells (Dimension 3100 AFM), and lymphoma patient cells (Dimension 3100 AFM). The imaging mode used was "contact mode", the scan force was 50 pN, and the scan rate was 1 Hz. Measurement of the CD20-Rituximab rupture forces was performed using the Dimension 3100 AFM. Approximately 500 force curves (at the same loading rate of 1.99 μm/s) were obtained for the CD20 proteins, Raji cells, and lymphoma patient B cells using force curve mode and functionalized probes. Blocking experiments [21] were used to verify the specific CD20-Rituximab binding forces. Free Rituximab was then added to mask the CD20 molecules on the substrate/cell, and force curve obtained gain about 30 min later.

2.5 Poisson analysis

Several CD20-Rituximab complexes may be formed during the process of obtaining the force curves. Therefore, Poisson analysis [22] was used to calculate individual CD20-Rituximab rupture forces using the following formula:

$$\frac{\sigma^2}{\mu} = F, \tag{1}$$

in which σ^2 and μ represent the variance and mean, respectively, for one measurement, and F is the binding force. If several measurements at the same loading rate are performed, the variance can be plotted against the mean. The individual CD20-Rituximab rupture force is equal to the slope of the fitted line.

3 Results and discussion

Figure 2 shows the results of measuring the rupture forces between purified CD20 proteins and Rituximab. After

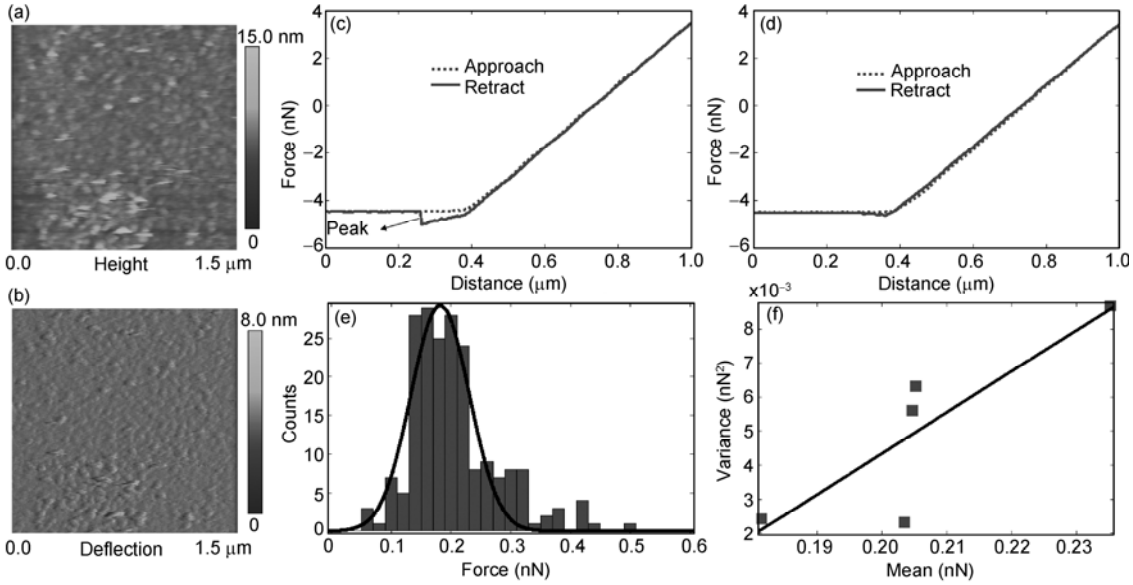

Figure 2 Measurement of the rupture force between purified CD20 proteins and Rituximab. (a) AFM contact mode topography image of CD20 proteins. (b) AFM contact mode deflection image of CD20 protein. (c) A typical force curve. (d) Force curve after adding free Rituximab. (e) Histogram showing the rupture forces. (f) Poisson analysis was used to calculate the individual rupture forces.

treating the mica with APTES and glutaraldehyde, the exposed aldehydes react with the lysine residues [18]. The CD20 proteins contain lysine residues and, therefore, are cross-linked onto the mica. Figure 2(a) and (b) shows the AFM contact mode images obtained for the purified CD20 proteins. The scan size was 1.5 μm. Figure 2(a) shows the topography image and Figure 2(b) shows the deflection image. Many CD20 protein particles can be seen distributed over the mica surface. A prerequisite of imaging proteins in fluids is their attachment to a flat support [23]; mica is the most commonly used support because of its atomically flat surface and ease of preparation [24]. However, the intrinsic hydrophobicity of proteins means that they are difficult to attach to mica, which is hydrophilic [25]. Various methods, including physical adsorption and covalent attachment, have been used to attach proteins to mica surfaces [26]. Henderson et al. [25] imaged individual ROMK1 proteins by coating the mica with cetylpyridinium chloride, and Kada et al. [27] used AFM to visualize individual ryanodine receptors adsorbed onto mica surfaces in the presence of Ca^{2+}. Wang et al. [28] imaged IgG_4 proteins by treating the mica with APTES and glutaraldehyde. However, because of the soft, fragile, corrugated and dynamic nature of the cell surface, visualizing the topography of individual receptors on living mammalian cells is still a challenge [29], and co-operation between experts from different scientific disciplines is essential to achieve this goal.

A typical force curve obtained using CD20-coated mica and a Rituximab-conjugated a probe is shown in Figure 2(c). The dotted line indicates the approach process and the solid line indicates the retraction process. An abrupt peak is visible on the retract curve. When performing the functionalization experiments, the bonds between AFM tip and PEG linker molecule, the bonds between Rituximab and the PEG linker molecule, and the bonds between the CD20 and the substrate should be much stronger than the bonds between CD20 and Rituximab. Research indicates that the bonds between the NHS end of the PEG linker and the AFM tip are much stronger than protein-protein interactions [10,21]. Additionally, the bonds between the MAL end of the PEG linker and the antibody, and the bonds between proteins and the aldehyde group on the functionalized mica are much stronger than protein-protein interactions [20,28]. Therefore, during the process of stretching the CD20-Rituximab complex in the force curve mode, the CD20-Rituximab complex ruptures first. When force curves were obtained again after adding free Rituximab, no peaks were visible on the retract curve (Figure 2(d)). This confirmed that the peak in Figure 2(c) corresponded to the specific binding between CD20 proteins on the mica and the Rituximab on the AFM tip. After calculating the rupture forces for each force curve obtained on the mica, a histogram of the rupture forces was constructed (Figure 2(e)). Gaussian fitting of the histogram indicated that the rupture force was 182±69 pN. The mean and variance were calculated for 5 measurements. The means were 0.2053, 0.1814, 0.2035, 0.2353, and 0.2047, and the variances were 0.0063, 0.0024, 0.0023, 0.0087, and 0.0056. The fitting function used was $f(x) = p_1 \times x + p_2$, and the results indicated that $p_1 = 0.1205$ and $p_2 = -0.01977$. The slope of the fitting line indicated that the individual rupture force was 121 pN (Figure 2(f)).

Figure 3 shows the rupture forces between CD20 proteins expressed by Raji cells and Rituximab. Figure 3(a) shows the contact mode topography image. The scan size

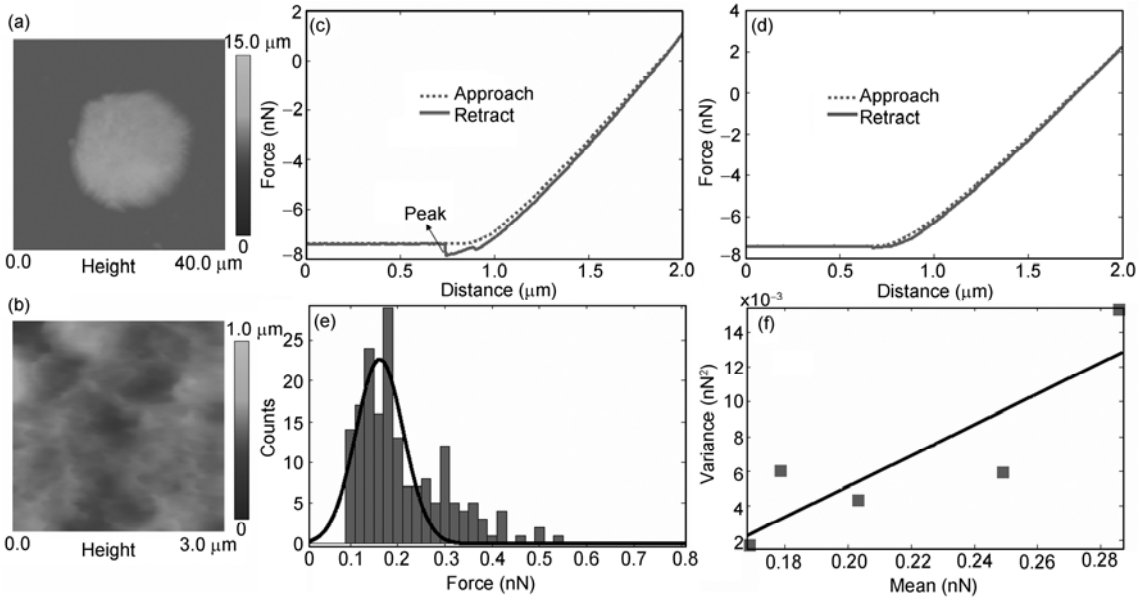

Figure 3 Measurement of the rupture force between CD20 proteins on Raji cells and Rituximab. (a) AFM contact mode topography image of Raji cells. (b) AFM contact mode topography image of the local area of the Raji cell. (c) A typical force curve. (d) Force curve after adding free Rituximab. (e) Histogram of the rupture forces. (f) Poisson analysis was used to calculate the individual rupture forces.

was 40 μm. To visualize the topography of the local cell surface, the scan size was reduced to 3 μm. Figure 3(b) shows the topography image of the local area. From these images, it can be seen that the cell surface is corrugated and rough. A typical force curve obtained using Raji cells and a Rituximab-conjugated probe is shown in Figure 3(c). There is an abrupt peak on the retract curve, which disappears after the addition of free Rituximab (Figure 3(d)). This confirmed the specific CD20-Rituximab binding interactions. Figure 3(e) shows the histogram of the rupture forces. Gaussian fitting indicated that the rupture force was 162±71 pN. For five individual measurements, the means were 0.1787, 0.2859, 0.2033, 0.1690, and 0.2493, and the variances were 0.0060, 0.0153, 0.0043, 0.0017, and 0.0059. The fitting function used was $f(x) = p_1 \times x + p_2$ and the fitting results indicated that $p_1 = 0.08888$ and $p_2 = -0.01267$. The slope of the fitted line on the plot of variance against the mean indicated that the individual rupture force was 89 pN (Figure 3(f)).

Figure 4 shows the results of measuring the rupture forces between CD20 proteins on lymphoma patient B cells and Rituximab. Figure 4(a) and (b) shows the contact mode AFM images of lymphoma patient cells. Figure 4(a) shows the topography image and Figure 4(b) shows the deflection image. The scan size was 50 μm. Many red blood cells can be seen among the patient cells. CD20 is expressed on B cells, but not expressed on red blood cells. To measure the CD20-Rituximab rupture forces on patient B cells, the functionalized probe was first used to scan a large area (Figure 4(c)). Then, several cells were randomly selected and force curves obtained. If no abrupt peaks were visible in the force curves obtained for an individual cell (Figure 4(c), I), the cell was discarded. If abrupt peaks were visible in the force curves (Figure 4(c), II and III), the cell was selected and the CD20-Rituximab rupture forces were measured (about 100 force curves were obtained). The inset in Figure 4(d) shows a histogram of the rupture forces. Gaussian fitting indicated that the rupture force was 180±90 pN. For 6 measurements, the means were 0.1302, 0.1981, 0.2204, 0.2909, 0.4548, and 0.4936, and the variances were 0.0044, 0.0082, 0.0183, 0.029, 0.0403, and 0.0529. The fitting function used was $f(x) = p_1 \times x + p_2$ and the fitting results indicated that $p_1 = 0.1259$ and $p_2 = -0.01199$. The slope of the fitted line on the plot of variance against the mean indicated that the individual rupture force was 126 pN (Figure 4(d)).

After analyzing and measuring the CD20-Rituximab rupture forces on purified CD20 proteins, CD20 proteins on Raji cells, and CD20 proteins on lymphoma patient B cells, we can see that the rupture force of the purified CD20 proteins was 182±69 pN, that of the CD20 proteins on Raji cells was 162±71 pN, and that of the CD20 proteins on lymphoma patient B cells was 180±90 pN. As mentioned above, several CD20-Rituximab complexes may form during the measurement process and, after Poisson analysis, the individual CD20-Rituximab rupture forces for the purified CD20 proteins, CD20 proteins on Raji cells, and CD20 proteins on lymphoma patient B cells were calculated to be 121, 89, and 126 pN, respectively. Combing the histogram results and Poisson analysis results shows that the rupture force for CD20 proteins on Raji cells was the lowest, and the rupture force for the purified CD20 proteins was similar to that for CD20 proteins on lymphoma patient B cells. It should be noted that the Raji cells were cultured *in vitro*, and it is known that cells grown in a flat 2-D environments

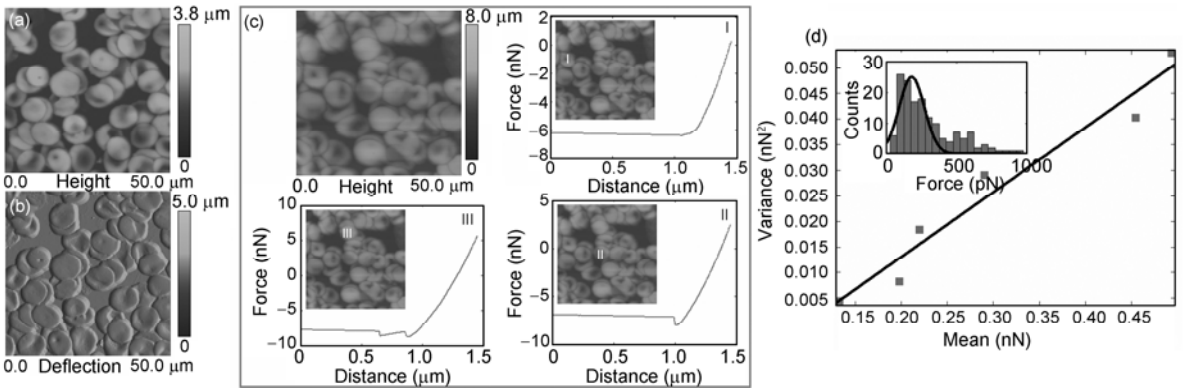

Figure 4 Measurement of the rupture force between CD20 proteins on the lymphoma patient cells and Rituximab. (a) AFM contact mode topography image of patient cells. (b) AFM contact mode deflection image of patient cells. (c) Method of measuring the CD20-Rituximab rupture forces on patient cells. (d) Poisson analysis was used to calculate the individual rupture force. (Inset) histogram showing the rupture forces.

differ considerably their structure and function from those grown in a 3-D *in vivo* environments [30]. This may be why the rupture forces for CD20 proteins on Raji cells and the CD20 proteins on patient B cells were different in this study. Additionally, CD20 proteins expressed on prokaryotic cells *in vitro* do not completely correspond to natural human CD20 proteins *in vivo*. For mammalian proteins, a mammalian expression system is likely to give the best results in terms of protein structure and function [31]. The difference between the *in vitro* and *in vivo* environment may result in differences between proteins, and these differences may account for the rupture forces measured for the purified CD20 proteins and CD20 proteins on Raji cells. These results indicate that, if we are to thoroughly investigate the mechanisms underlying the variable efficacy of Rituximab, experiments should be performed using cells from lymphoma patients. Recently, AFM research on patient cells indicated that the distribution of CD20 molecules on B cells from healthy volunteers was uniform, whereas that on B cells from B-CLL patients was relatively sparse [32]. Gu et al. [33] suggested that the binding force between CD20 and anti-CD20 is closely associated with the linker peptide. However, the *in vivo* mechanism of action of Rituximab is still unknown [15], knowledge a regarding its variable efficacy is scarce, and further study is required to elucidate the underlying mechanisms.

4 Conclusions

More effective, targeted drugs are urgently needed for Rituximab-targeted therapy of B-cell non-Hodgkin's lymphoma because of the variable efficacy observed between lymphoma patients. AFM SMFS provides a new method for investigating specific molecular interactions and can be used to obtain new knowledge about the molecular interactions at the level of individual cells/molecules. The rupture forces between Rituximab and purified CD20 proteins, CD20 proteins on Raji cells, and CD20 proteins on lymphoma patient B cells were measured using AFM SMFS and the differences between the rupture forces analyzed. In addition, the topography of the purified CD20 proteins, Raji cells, and lymphoma patient B cells was visualized. The results indicated that the rupture force between CD20 proteins on Raji cells and Rituximab was the lowest (89 pN), whereas that between purified CD20 proteins (121 pN) was similar to that for the CD20 proteins on lymphoma patient B cells (126 pN). These results provide the foundation for further investigations into the molecular mechanism underlying the variable efficacy of Rituximab, and may provide a key technology that can be used to develop the next generation of monoclonal antibody drugs.

This work was supported by the National Natural Science Foundation of China (60904095), National High Technology Research and Development Program of China (2009AA03Z316), and CAS FEA International Partnership Program for Creative Research Teams.

1 Binnig G, Quate C F, Gerber C. Atomic force microscope. Phys Rev Lett, 1986, 56: 930–933
2 Dufrene Y F. Atomic force microscopy and chemical force microscopy of microbial cells. Nat Protoc, 2008, 3: 1132–1138
3 Dufrene Y F. Using nanotechniques to explore microbial surfaces. Nat Rev Microbiol, 2004, 2: 451–460
4 Muller D J, Dufrene Y F. Atomic force microscopy as a multifunctional molecular toolbox in nanobiotechnology. Nat Nanotechnol, 2008, 3: 261–269
5 Chen P P, Dong H T, Chen L, et al. Application of atomic force microscopy to living samples from cells to fresh tissues. Chinese Sci Bull, 2009, 54: 2410–2415
6 Li M, Liu L Q, Xi N, et al. Imaging and mechanical property measurement of the lymphoma cells by atomic force microscopy (in Chinese). Chinese Sci Bull (Chinese Ver.), 2010, 55: 2188–2196
7 Dufrene Y F, Evans E, Engel A, et al. Five challenges to bringing single-molecule force spectroscopy into living cells. Nat Methods, 2011, 8: 123–127
8 Muller D J, Helenius J, Alsteens D, et al. Force probing surfaces of living cells to molecular resolution. Nat Chem Biol, 2009, 5: 383–390
9 Florin E L, Moy V T, Gaub H E. Adhesion forces between individual

ligand-receptor pairs. Science, 1994, 264: 415–417
10 Hinterdorfer P, Baumgartner W, Gruber H J, et al. Detection and localization of individual antibody-antigen recognition events by atomic force microscopy. Proc Natl Acad Sci USA, 1996, 93: 3477–3481
11 Puntheeranurak T, Wildling L, Gruber H J, et al. Ligands on the string:single-molecule AFM studies on the interaction of antibodies and substrates with the Na^+-glucose co-transporter SGLT1 in living cells. J Cell Sci, 2006, 119: 2960–2967
12 Shi X, Xu L, Yu J, et al. Study of inhibition effect of Herceptin on interaction between Heregulin and ErbB receptors HER3/HER2 by single-molecule force spectroscopy. Exp Cell Res, 2009, 315: 2847–2855
13 Beers S A, French R R, Chan H T C, et al. Antigenic modulation limits the efficacy of anti-CD20 antibodies: Implications for antibody selection. Blood, 2010, 115: 5191–5201
14 Glennie M J, French R R, Cragg M S, et al. Mechanisms of killing by anti-CD20 monoclonal antibodies. Mol Immunol, 2007, 44: 3823–3837
15 Cartron G, Watier H, Golay J, et al. From the bench to the bedside: Ways to improve Rituximab efficacy. Blood, 2004, 104: 2635–2642
16 Lim S H, Beers S A, French R R, et al. Anti-CD20 monoclonal antibodies: Historical and future perspectives. Haematologica, 2010, 95: 135–143
17 Li B, Zhao L, Guo H, et al. Characterization of a Rituximab variant with potent antitumor activity against Rituximab-resistant B-cell lymphoma. Blood, 2009, 114: 5007–5015
18 Wang H, Bash R, Yodh J G, et al. Glutaraldehyde modified mica: A new surface for atomic force microscopy of chromatin. Biophys J, 2002, 83: 3619–3625
19 Stroh C, Wang H, Bash R, et al. Single-molecule recognition imaging microscopy. Proc Natl Acad Sci USA, 2004, 101: 12503–12507
20 Ebner A, Wildling L, Kamruzzahan A S M, et al. A new, simple method for linking of antibodies to atomic force microscopy tips. Bioconjugate Chem, 2007, 18: 1176–1184
21 Hinterdorfer P, Dufrene Y F. Detection and localization of single molecular recognition events using atomic force microscopy. Nat Methods, 2006, 3: 347–355
22 Stevens F, Lo Y S, Harris J M, et al. Computer modeling of atomic force microscopy force measurements: Comparisons of Poisson, histogram, and continuum methods. Langmuir, 1999, 15: 207–213
23 Kada G, Kienberger F, Hinterdorfer P. Atomic force microscopy in bionanotechnology. Nano Today, 2008, 3: 12–19
24 Muller D J, Engel A, Amrein M. Preparation techniques for the observation of native biological systems with the atomic force microscope. Biosens Bioelectron, 1997, 12: 867–877
25 Henderson R M, Schneider S, Li Q, et al. Imaging ROMK1 inwardly rectifying ATP-sensitive K^+ channel protein using atomic force microscopy. Proc Natl Acad Sci USA, 1996, 93: 8756–8760
26 Kirat K E, Burton I, Dupres V, et al. Sample preparation procedures for biological atomic force microscopy. J Microsc, 2005, 218: 199–207
27 Kada G, Blayney L, Jeyakumar L H, et al. Recognition force microscopy/spectroscopy of ion channels: Applications to the skeletal muscle Ca^{2+} release channel (RYR1). Ultramicroscopy, 2001, 86: 129–137
28 Wang H, Kutner L O, Lin M, et al. Imaging glycosylation. J Am Chem Soc, 2008, 130: 8154–8155
29 Muller D J, Dufrene Y F. Force nanoscopy of living cells. Curr Biol, 2011, 21: R212–R216
30 Yamada K M, Cukierman E. Modeling tissue morphogenesis and cancer in 3D. Cell, 2007, 130: 601–610
31 Werten P J L, Remigy H W, Groot B L, et al. Progress in the analysis of membrane protein structure and function. FEBS Lett, 2002, 529: 65–72
32 Wang Q, Lu Y, Li S, et al. Distribution and force spectroscopy of CD20 antigen-antibody binding on the B cell surface (in Chinese). Chin J Biotech, 2011, 27: 131–136
33 Gu X, Jia X, Feng J, et al. Molecular modeling and affinity determination of scFv antibody: Proper linker peptide enhances its activity. Ann Biomed Eng, 2010, 38: 537–549